IRIS AperTO

UNIVERSITÀ DEGLI STUDI DI TORINO

AperTO - Archivio Istituzionale Open Access dell'Università di Torino

Adaptive procedures for meshfree RBF unsymmetric and symmetric collocation methods

This is the author's manuscript

Original Citation:

Availability:

This version is available http://hdl.handle.net/2318/1739810 since 2020-07-18T16:59:01Z

Published version:

DOI:10.1016/j.amc.2020.125354

Terms of use:

Open Access

Anyone can freely access the full text of works made available as "Open Access". Works made available under a Creative Commons license can be used according to the terms and conditions of said license. Use of all other works requires consent of the right holder (author or publisher) if not exempted from copyright protection by the applicable law.

(Article begins on next page)

08 August 2024

IRIS AperTO

UNIVERSITÀ DEGLI STUDI DI TORINO

This is the author's final version of the contribution published as:

Roberto Cavoretto, Alessandra De Rossi. Adaptive refinement procedures for meshless RBF unsymmetric and symmetric collocation methods. *Applied Mathematics and Computation 382 (2020), 125354, DOI: 10.1016/j.amc.2020.125354.*

The publisher's version is available at:
[https://doi.org/10.1016/j.amc.2020.125354]

When citing, please refer to the published version.

Link to this full text:
[http://hdl.handle.net/2318/1739810]

This full text was downloaded from iris-AperTO: https://iris.unito.it/

iris-AperTO

University of Turin's Institutional Research Information System and Open Access Institutional Repository

Adaptive procedures for meshfree RBF unsymmetric and symmetric collocation methods

Roberto Cavoretto[a,b], Alessandra De Rossi[a,b]

[a] *Department of Mathematics "Giuseppe Peano", University of Torino, via Carlo Alberto 10, 10123 Torino, Italy*
[b] *Member of the INdAM Research group GNCS*

Abstract

In this article we present an adaptive scheme for solving radial basis function collocation problems, which involve elliptic partial differential equations. The proposed algorithm is applied to two usual numerical methods, known as the nonsymmetric Kansa's method and the symmetric Hermite-based approach. Basically, the refinement algorithm is firstly characterized by the use of an adaptive superimposition scheme, in which an error estimate compares two approximate solutions computed on a coarser and a finer set of collocation points, and then on a modified adaptive residual subsampling scheme. Blending these computational techniques we detect the areas that need to be refined, also having the chance to further add and/or remove adaptively collocation points. Our study is supported by several numerical results, which illustrate the performance of our iterative algorithm.

Keywords: meshfree approximation, adaptive algorithms, refinement schemes, collocation methods, partial differential equations
2010 MSC: 65D15, 65M70

1. Introduction

Over the last years meshfree methods have been gaining more and more importance and recognition from applied mathematicians and engineers since they are powerful and effective numerical tools that enable us to solve various types of problems in approximation theory and in the field of partial differential equations (PDEs). In particular, collocation methods involving the use of radial basis functions (RBF) or kernels have constantly being studied and developed to effectively model science and engineering problems (see e.g. [15, 22]). Compared to some traditional numerical methods such as finite differences, finite volumes and boundary elements, the RBF collocation methods have many remarkable advantages. Such approaches can indeed be easily implemented even in high dimensions and with complex domain geometries, and can also get high convergence orders (see [11, 13]). Nevertheless, in literature RBF methods are known to suffer from ill-conditioning, mainly when a large number of collocation points are involved and accordingly the size of the resulting matrix system grows. For this reason, the need of designing new adaptive numerical algorithms that enable to achieve a certain level of accuracy with the minimum number of points motivates our research (see e.g. [3, 6, 16, 18, 27]). Moreover, we remark as – unlike the above-mentioned numerical methods – in the context of meshfree RBF methods the number of works regarding this topic is relatively reduced; for further details see [7, 8, 23, 25, 29].

In this paper we propose a new adaptive refinement algorithm to model elliptic PDEs. To analyze the behavior of our numerical scheme, we focus on two collocation RBF approaches, namely the nonsymmetric Kansa's method [17] and the symmetric Hermite-based one [9]. Both computational techniques have spawned

Email addresses: roberto.cavoretto@unito.it (Roberto Cavoretto), alessandra.derossi@unito.it (Alessandra De Rossi)

several works, mainly from people that commonly are scientifically active in several different research areas (see e.g. [11, 19, 30] and references therein). The iterative algorithm we propose here is characterized by two stages. The first stage consists in applying an *adaptive superimposition* (AS) refinement scheme, which is based on an error estimate that makes a comparison between two approximate RBF collocation solutions computed on a coarser and a finer set of discretization points. The second stage is instead distinguished by a *modified adaptive residual subsampling* (MARS) refinement procedure which is dependent from another error indicator. This approach enables us to further refine adaptively the collocation points on the basis of information deduced from the previous error estimate. In doing so, we are able to add points if they are missing and/or remove them when an excessive number of points is present. The resultant scheme consisting of two stages is thus denoted as AS-MARS. Several numerical experiments highlight the performance of the AS-MARS algorithm on some benchmark Poisson-type test problems, also showing how the procedures work when applying to Kansa's and Hermite-based methods. Finally, we conclude by observing that similar approaches consisting in the addition/removal of points can also be found in some recent works, where we used the RBF partition of unity (PU) collocation method (see [2, 3]). However, in those papers when the PDE solution presents quite steep variations, the RBF-PU method is not always able to get the expected precision. This fact motivated us to further investigate the mentioned issue by proposing new adaptive algorithms in RBF collocation framework. With this aim in [5] we thus proposed a first scheme based on the use of a Leave One Out Cross Validation technique, while a second approach is presented in the current manuscript.

The paper is organized as follows. In Section 2 we exhibit nonsymmetric and symmetric RBF collocation methods, which are used to solve numerically elliptic PDEs, introducing some basic notions regarding the theory of RBFs. In Section 3 we present the adaptive refinement algorithm based on the AS scheme and the MARS technique. Section 4 shows numerical results and illustrates the performance of our adaptive algorithm on some elliptic PDE problems. Finally, Section 5 contains conclusions and future work.

2. Meshfree methods for RBF collocation

Assuming that Ω is a domain in $\mathbb{R}^d$ and $\mathcal{L}$ is a linear elliptic partial differential operator, a generic (time independent) boundary value problem is given by the PDE

$$\mathcal{L}u(\boldsymbol{x}) = g_1(\boldsymbol{x}), \qquad \text{for } \boldsymbol{x} \in \Omega, \tag{1}$$

together with the related Dirichlet boundary conditions (BCs)

$$u(\boldsymbol{x}) = g_2(\boldsymbol{x}), \qquad \text{for } \boldsymbol{x} \in \partial\Omega. \tag{2}$$

In order to solve elliptic PDE problems via RBF collocation methods, we consider a nonsymmetric approach, also known as Kansa's method [17], and a symmetric one that is also often referred to as a Hermite-based method [9]. In doing so, we define the set $X_N = \{\boldsymbol{x}_1, \ldots, \boldsymbol{x}_N\} \subset \Omega$ of the so-called *collocation points* and the set $Z_N = \{\boldsymbol{z}_1, \ldots, \boldsymbol{z}_N\}$ of the so-called *centers*. For the sake of clarity, in what follows we will distinguish between interior and boundary collocation points and centers, denoting the corresponding sets with the subscripts N_I and N_B, respectively.

2.1. Kansa's collocation

In case of Kansa's collocation the numerical solution $\hat{u}$ is defined as a linear combination of RBFs [10]

$$\hat{u}(\boldsymbol{x}) = \sum_{j=1}^{N} c_j \phi_\varepsilon(||\boldsymbol{x} - \boldsymbol{z}_j||_2), \tag{3}$$

where $\phi_\varepsilon : \mathbb{R}_{\geq 0} \to \mathbb{R}$ is any radial kernel or RBF which is dependent from a *shape parameter* $\varepsilon > 0$, with $\phi_\varepsilon(r) = \phi(\varepsilon r)$, and the distance $r = ||\boldsymbol{x} - \boldsymbol{z}||_2$ expressed in 2-norm, for all $\boldsymbol{x}, \boldsymbol{z} \in \Omega$ (see Table 1, for details

RBF	$\phi_\varepsilon(r)$
Gaussian C^∞ (GA)	$\exp(-\varepsilon^2 r^2)$
Inverse MultiQuadric C^∞ (IMQ)	$\dfrac{1}{\sqrt{1+\varepsilon^2 r^2}}$
MultiQuadric C^∞ (MQ)	$\sqrt{1+\varepsilon^2 r^2}$
Matérn C^6 (M6)	$\exp(-\varepsilon r)(\varepsilon^3 r^3 + 6\varepsilon^2 r^2 + 15\varepsilon r + 15)$
Matérn C^4 (M4)	$\exp(-\varepsilon r)(\varepsilon^2 r^2 + 3\varepsilon r + 3)$

Table 1: Some examples of popular RBFs.

[1, 32]). The coefficients c_j in (3) are obtained by solving the following collocation system

$$\begin{bmatrix} \hat{\Phi}_{\mathcal{L}} \\ \hat{\Phi} \end{bmatrix} \boldsymbol{c} = \boldsymbol{t}, \tag{4}$$

where the entries in the two blocks of collocation matrix are given by

$$\begin{aligned} (\hat{\Phi}_{\mathcal{L}})_{ij} &= \mathcal{L}\phi_\varepsilon(||\boldsymbol{x}_i - \boldsymbol{z}_j||_2), \qquad \text{for } \boldsymbol{x}_i \in X_{N_I},\ \boldsymbol{z}_j \in Z_N, \\ \hat{\Phi}_{ij} &= \phi_\varepsilon(||\boldsymbol{x}_i - \boldsymbol{z}_j||_2), \qquad \text{for } \boldsymbol{x}_i \in X_{N_B},\ \boldsymbol{z}_j \in Z_N, \end{aligned}$$

and $\boldsymbol{t}$ is the vector consisting of entries

$$t_i = \begin{cases} g_1(\boldsymbol{x}_i), & \text{for } \boldsymbol{x}_i \in X_{N_I}, \\ g_2(\boldsymbol{x}_i), & \text{for } \boldsymbol{x}_i \in X_{N_B}. \end{cases} \tag{5}$$

Since the collocation matrix in (4) may be singular for certain configurations of the centers $\boldsymbol{z}_j$, this nonsymmetric approach could not be well-posed for some sets of centers (see [10, 14]). In any case, it is possible to find sufficient conditions on the centers so that invertibility of the matrix in (4) is guaranteed. Hence, based on theoretical convergence analysis of the nonsymmetric method in [21, 28], Kansa's method has gained popularity despite its potential failure when applying in its most straightforward and naive implementation [14]. In fact, one possible approach is to adaptively select good centers to ensure invertibility of the collocation matrix by means of an iterative scheme [26], or use refinement algorithms [5, 4].

2.2. Hermite-based collocation

The Hermite-based approach is derived from the corresponding generalized interpolation method (see e.g. [10]). Assuming to be given the elliptic PDE problem (1)–(2), we can indeed apply the results from generalized Hermite interpolation which ensure the non-singularity of the collocation matrix. In so doing, instead of using the expansion (3), we express the approximate solution $\hat{u}$ for the unknown function u as follows:

$$\hat{u}(\boldsymbol{x}) = \sum_{j=1}^{N_I} c_j \mathcal{L}^{\boldsymbol{z}} \phi_\varepsilon(||\boldsymbol{x} - \boldsymbol{z}_j||_2) + \sum_{j=N_I+1}^{N} c_j \phi_\varepsilon(||\boldsymbol{x} - \boldsymbol{z}_j||_2). \tag{6}$$

Here, the differential operator $\mathcal{L}^{\boldsymbol{z}}$ acts on the radial function ϕ_ε and has to be viewed as a function of $\boldsymbol{z}$. Moreover, we remark that in the second sum of the expansion (6) the index $j = N_I + 1, \ldots, N$ simply identifies the N_B boundary centers. Then, the coefficients c_j in (6) can be found by solving the linear system of the form

$$\begin{bmatrix} \hat{\Phi}_{\mathcal{L}\mathcal{L}^{\boldsymbol{z}}} & \hat{\Phi}_{\mathcal{L}} \\ \hat{\Phi}_{\mathcal{L}^{\boldsymbol{z}}} & \hat{\Phi} \end{bmatrix} \boldsymbol{c} = \boldsymbol{t}, \tag{7}$$

where the entries of the four blocks in the collocation matrix are

$$\begin{aligned}
(\hat{\Phi}_{\mathcal{L}\mathcal{L}^{\boldsymbol{z}}})_{ij} &= \mathcal{L}\phi_\varepsilon(||\boldsymbol{x}_i - \boldsymbol{z}_j||_2), && \boldsymbol{x}_i \in X_{N_I},\ \boldsymbol{z}_j \in Z_{N_I},\\
(\hat{\Phi}_{\mathcal{L}})_{ij} &= \mathcal{L}\phi_\varepsilon(||\boldsymbol{x}_i - \boldsymbol{z}_j||_2), && \boldsymbol{x}_i \in X_{N_I},\ \boldsymbol{z}_j \in Z_{N_B},\\
(\hat{\Phi}_{\mathcal{L}^{\boldsymbol{z}}})_{ij} &= \mathcal{L}^{\boldsymbol{z}}\phi_\varepsilon(||\boldsymbol{x}_i - \boldsymbol{z}_j||_2), && \boldsymbol{x}_i \in X_{N_B},\ \boldsymbol{z}_j \in Z_{N_I},\\
\hat{\Phi}_{ij} &= \phi_\varepsilon(||\boldsymbol{x}_i - \boldsymbol{z}_j||_2), && \boldsymbol{x}_i \in X_{N_B},\ \boldsymbol{z}_j \in Z_{N_B},
\end{aligned}$$

and the vector $\boldsymbol{t}$ is defined as in (5). Hence, when the set Z_N coincides with X_N, we have the symmetric matrix in (7) and the collocation approach is definitely well-posed. Moreover, we can give the following convergence result [10, 32]:

Theorem 2.1. *Let $\Omega \subseteq \mathbb{R}^d$ be a polygonal and open region. Let $\mathcal{L} \neq 0$ be a second-order linear elliptic differential operator with coefficients in $C^{2(k-2)}(\bar{\Omega})$ that either vanish on $\bar{\Omega}$ or have no zero there. Suppose that $\phi \in C^{2k}(\mathbb{R}^d)$ is a strictly positive definite function. Suppose further that the boundary value problem*

$$\begin{aligned}
\mathcal{L}u &= g_1 \qquad \text{in } \Omega,\\
u &= g_2 \qquad \text{on } \partial\Omega
\end{aligned}$$

is uniquely solvable. In particular, the solution $u \in \mathcal{N}_\Phi(\Omega)$ for some $g_1 \in C(\Omega)$ and $g_2 \in C(\partial\Omega)$, where $\mathcal{N}_\phi$ denotes the native space. Then, if $\hat{u}$ is the approximate solution in (6)*, we get*

$$||u - \hat{u}||_{L_\infty(\Omega)} \leq Ch^{k-2}||u||_{\mathcal{N}_\phi(\Omega)}$$

for all sufficiently small h, where $h = \sup_{\boldsymbol{x}\in\Omega} \min_{\boldsymbol{x}_i \in X_N} ||\boldsymbol{x} - \boldsymbol{x}_i||_2$ defines the fill distance, namely the larger of the distances in the interior and on the boundary of Ω, respectively.

3. Adaptive refinement algorithm

In this section we present our new adaptive refinement algorithm, which is composed of two stages. The first phase consists in applying the AS scheme, where we compare two approximate solutions of the form (3) (or (6)) computed on a coarser and a finer set of collocation points, thus generating an error estimate. This process enables us to detect and refine the regions of the domain Ω that do not give us accurate enough results. The second phase is characterized by a further refinement technique based on the MARS method. The latter also depends on an error estimate, which allows us to add/remove some points on the basis of information extracted from the estimator.

3.1. Refinement technique based on the AS scheme

At first, we define two initial sets $X^1_{N_1^{(1)}} = \{\boldsymbol{x}_1^{(1)}, \ldots, \boldsymbol{x}_{N_1^{(1)}}^{(1)}\}$ and $X^1_{N_2^{(1)}} = \{\boldsymbol{x}_1^{(1)}, \ldots, \boldsymbol{x}_{N_2^{(1)}}^{(1)}\}$ of collocation points and two initial sets $Z^1_{N_1^{(1)}} = \{\boldsymbol{z}_1^{(1)}, \ldots, \boldsymbol{z}_{N_1^{(1)}}^{(1)}\}$ and $Z^1_{N_2^{(1)}} = \{\boldsymbol{z}_1^{(1)}, \ldots, \boldsymbol{z}_{N_2^{(1)}}^{(1)}\}$ of centers. $X^1_{N_1^{(1)}}$ and $Z^1_{N_1^{(1)}}$ represent coarser sets, while $X^1_{N_2^{(1)}}$ and $Z^1_{N_2^{(1)}}$ are finer ones. This means that $N_1^{(1)} < N_2^{(1)}$, where the symbol $^{(1)}$ identifies the iteration number. For our purposes, it is useful to split the sets $X^1_{N_i^{(1)}}$ and $Z^1_{N_i^{(1)}}$, with $i = 1, 2$, as follows:

- $X^1_{N_{I_i}^{(1)}} = \{\boldsymbol{x}_1^{(1)}, \ldots, \boldsymbol{x}_{N_{I_i}^{(1)}}^{(1)}\}$ and $X^1_{N_{B_i}^{(1)}} = \{\boldsymbol{x}_1^{(1)}, \ldots, \boldsymbol{x}_{N_{B_i}^{(1)}}^{(1)}\}$ are sets of interior and boundary collocation points, respectively;
- $Z^1_{N_{I_i}^{(1)}} = \{\boldsymbol{z}_1^{(1)}, \ldots, \boldsymbol{z}_{N_{I_i}^{(1)}}^{(1)}\}$ and $Z^1_{N_{B_i}^{(1)}} = \{\boldsymbol{z}_1^{(1)}, \ldots, \boldsymbol{z}_{N_{B_i}^{(1)}}^{(1)}\}$ are sets of interior and external boundary centers, respectively.

Specifically, as evoked in [12], in this work we take $Z^1_{N^{(1)}_{I_i}} = X^1_{N^{(1)}_{I_i}}$ whereas $Z^1_{N^{(1)}_{B_i}}$ represents a set of centers that lies outside the domain Ω. However, we notice that the number of outside centers, whose we refer to as external boundary centers, is the same as boundary collocation points. Moreover, though our iterative process is basically completely general, we choose to begin with two initial sets of grid interior and boundary points, because this assumption allows us to uniformly cover the domain Ω detecting in a better way which areas of Ω need to be refined. In addition, we highlight that as in the above-mentioned sets $X^1_{N^{(1)}_1}$, $X^1_{N^{(1)}_2}$, $Z^1_{N^{(1)}_1}$ and $Z^1_{N^{(1)}_2}$ the superscript ^{1} refers to the first stage of the adaptive algorithm.

Then, the iterative procedure starts and, for $k = 1, 2, \ldots$, the collocation solutions $\hat{u}_{N^{(k)}_1}$ and $\hat{u}_{N^{(k)}_2}$ of the form (3) (or (6)) are computed on $N^{(k)}_1$ and $N^{(k)}_2$ collocation points and centers. In order to know where we need to refine, we compare the two approximate RBF solutions evaluated at the (coarser) set $X^1_{N^{(k)}_1}$, supposing that the solution computed on the (finer) set $X^1_{N^{(k)}_2}$ gives us more accurate results than the ones obtained by using the previous one. So we can define the following error indicator given by

$$E^{(k)}_i = |\hat{u}_{N^{(k)}_2}(\boldsymbol{x}^{(k)}_i) - \hat{u}_{N^{(k)}_1}(\boldsymbol{x}^{(k)}_i)|, \qquad \boldsymbol{x}^{(k)}_i \in X^1_{N^{(k)}_1}. \tag{8}$$

After fixing a tolerance τ, we detect all points $\boldsymbol{x}^{(k)}_i \in X^1_{N^{(k)}_1}$ such that

$$E^{(k)}_i > \tau. \tag{9}$$

To refine the distribution of discretization points, we compute the *separation distance*

$$q_{X^{(k)}_{N_1}} = \frac{1}{2} \min_{i \neq j} ||\boldsymbol{x}^{(k)}_i - \boldsymbol{x}^{(k)}_j||_2, \qquad \boldsymbol{x}^{(k)}_i \in X^1_{N^{(k)}_1}, \tag{10}$$

and, afterwards, for $k = 1, 2, \ldots$, we update the sets $X^1_{N^{(k+1)}_1}$ and $X^1_{N^{(k+1)}_2}$ of collocation points and the sets $Z^1_{N^{(k+1)}_1}$ and $Z^1_{N^{(k+1)}_2}$ of centers. In particular, if the condition (9) is satisfied, we add to $\boldsymbol{x}^{(k)}_i$ four and eight points to generate the sets $X^1_{N^{(k+1)}_1}$ and $X^1_{N^{(k+1)}_2}$, respectively (see Figure 1, top, left to right). Nevertheless, when $\boldsymbol{x}^{(k)}_i$ is on or near to the boundary, we reduce the number of points to be added (see Figure 1, bottom, left to right). In both cases the new sets are obtained by either adding or subtracting the value of (10) to the components of $\boldsymbol{x}^{(k)}_i$. Finally, the adaptive algorithm stops when there are no points anymore that satisfy the condition (9), returning the sets $X^1_{N^{(k^*)}_2}$ and $Z^1_{N^{(k^*)}_2}$, with k^* denoting the last iteration. A pseudo-code of this first stage is given in Procedure 1.

3.2. Refinement technique based on the MARS method

At the second stage of the algorithm we further refine the collocation points on the basis of the information deriving from a new error indicator. Here, this refinement phase is a sort of extension of the residual subsampling method proposed in [8], and later suitably modified for a RBF-PU collocation method [2, 3]. Basically, our computational technique is obtained through a good combination between an error indicator and a refinement procedure, which consists in solving, estimating and lastly adding or removing adaptively any points in the areas identified by the error indicator.

Therefore, we start from the output of the previous stage described in Procedure 1, denoting those final sets $X^1_{N^{(k^*)}_2}$ as $X^2_{N^{(1)}}$ and $Z^1_{N^{(k^*)}_2}$ as $Z^2_{N^{(1)}}$, i.e. we set $X^2_{N^{(1)}} = X^1_{N^{(k^*)}_2}$ and $Z^2_{N^{(1)}} = Z^1_{N^{(k^*)}_2}$, where the superscript ^{2} denotes now the second stage of our adaptive process. Then, for $k = 1, 2, \ldots$, we compute iteratively two collocation solutions of the form (3) (or (6)), called $\hat{u}$ and $\hat{u}^e$, respectively. Moreover, we remark that the above-mentioned sets can be split as follows: $X^2_{N^{(k)}} = X^2_{N^{(k)}_I} \cup X^2_{N^{(k)}_B}$ and $Z^2_{N^{(k)}} = Z^2_{N^{(k)}_I} \cup Z^2_{N^{(k)}_B}$. Therefore, we need to find the two approximate solutions $\hat{u}$ and $\hat{u}^e$, which are given by

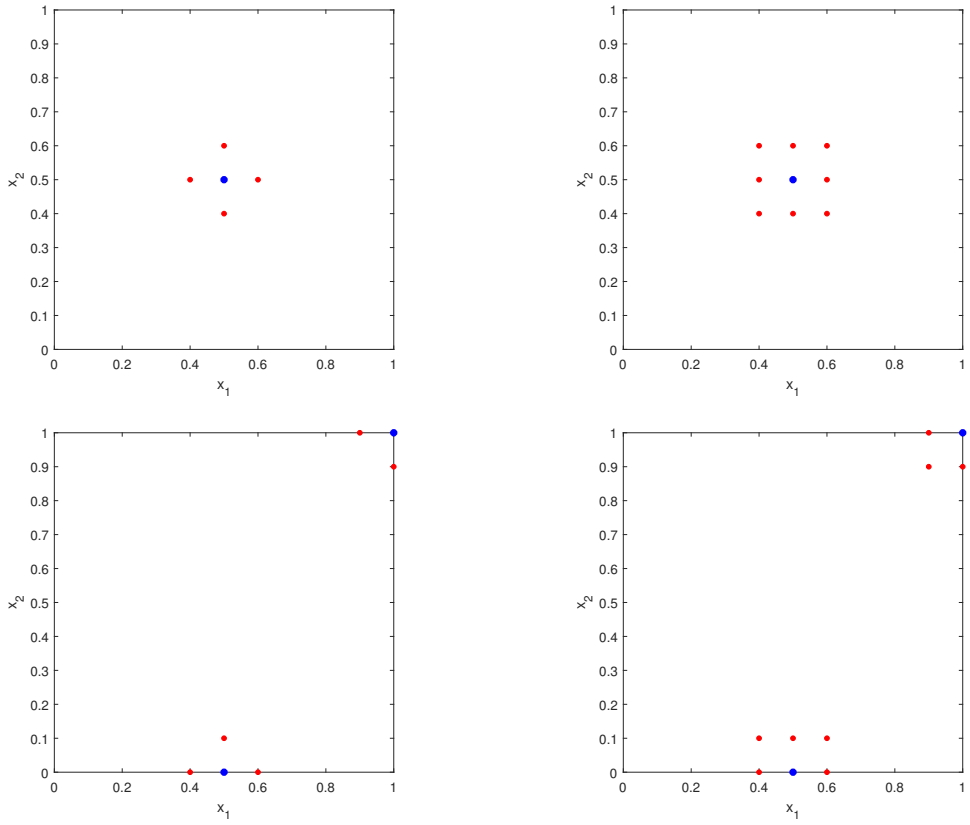

Figure 1: Example of refinement around the point $\boldsymbol{x}_i^{(k)}$, marked by a blue dot, to generate the new sets $X_{N_1^{(k+1)}}$ (left) and $X_{N_2^{(k+1)}}$ (right).

solving two linear systems of the form (4) (or (7)). For the sake of brevity, here we only deal with the case of Kansa's method but, similarly, it can also be applied to the Hermite one. Firstly, in order to determine $\hat{u}$, we construct a first system on coincident sets of collocation points and centers, i.e., we take $Z^2_{N^{(k)}} = X^2_{N^{(k)}}$, where k here is fixed. So the collocation matrix in (4) becomes

$$\begin{bmatrix} \hat{\Phi}_{\mathcal{L}} \\ \hat{\Phi} \end{bmatrix} = \begin{bmatrix} \hat{\Phi}_{\mathcal{L}_{II}} & \hat{\Phi}_{\mathcal{L}_{IB}} \\ \hat{\Phi}_{BI} & \hat{\Phi}_{BB} \end{bmatrix}, \tag{11}$$

where

$$\begin{aligned}
(\hat{\Phi}_{\mathcal{L}_{II}})_{ij} &= \mathcal{L}\phi_\varepsilon(||\boldsymbol{x}_i^{(k)} - \boldsymbol{z}_j^{(k)}||_2), && \boldsymbol{x}_i^{(k)} \in X^2_{N_I^{(k)}},\ \boldsymbol{z}_j^{(k)} \in Z^2_{N_I^{(k)}}, \\
(\hat{\Phi}_{\mathcal{L}_{IB}})_{ij} &= \mathcal{L}\phi_\varepsilon(||\boldsymbol{x}_i^{(k)} - \boldsymbol{z}_j^{(k)}||_2), && \boldsymbol{x}_i^{(k)} \in X^2_{N_I^{(k)}},\ \boldsymbol{z}_j^{(k)} \in Z^2_{N_B^{(k)}}, \\
(\hat{\Phi}_{BI})_{ij} &= \phi_\varepsilon(||\boldsymbol{x}_i^{(k)} - \boldsymbol{z}_j^{(k)}||_2), && \boldsymbol{x}_i^{(k)} \in X^2_{N_B^{(k)}},\ \boldsymbol{z}_j^{(k)} \in Z^2_{N_I^{(k)}} \\
(\hat{\Phi}_{BB})_{ij} &= \phi_\varepsilon(||\boldsymbol{x}_i^{(k)} - \boldsymbol{z}_j^{(k)}||_2), && \boldsymbol{x}_i^{(k)} \in X^2_{N_B^{(k)}},\ \boldsymbol{z}_j^{(k)} \in Z^2_{N_B^{(k)}}.
\end{aligned} \tag{12}$$

Secondly, to find the approximate solution $\hat{u}^e$, we have to define a second system. In doing that, for each iteration k, we use the same set $X^2_{N^{(k)}} = X^2_{N_I^{(k)}} \cup X^2_{N_B^{(k)}}$ of collocation points as for $\hat{u}$, whereas we split the set of centers as $Z^2_{N^{(1)}} = Z^2_{N_I^{(k)}} \cup Z^{2,e}_{N_B^{(k)}}$, where $Z^{2,e}_{N_B^{(k)}}$ denotes the external boundary centers previously

Procedure 1: Refinement technique based on the AS scheme

STEP 1 Generate two initial sets $X^1_{N_1^{(1)}}$ and $X^1_{N_2^{(1)}}$ of collocation points

and two initial sets $Z^1_{N_1^{(1)}}$ and $Z^1_{N_2^{(1)}}$ of centers, with $N_1^{(1)} < N_2^{(1)}$

STEP 2 Fix a tolerance $\tau > 0$

STEP 3 For $k = 1, 2, \ldots$ compute the collocation solutions $\hat{u}_{N_1^{(k)}}$ and $\hat{u}_{N_2^{(k)}}$ via (3) (or (6))

constructed on the coarser sets $X^1_{N_1^{(k)}}$ and $Z^1_{N_1^{(k)}}$, and the finer ones $X^1_{N_2^{(k)}}$ and $Z^1_{N_2^{(k)}}$

STEP 4 Evaluate the error indicator (8) at the point $\boldsymbol{x}_i^{(k)} \in X^1_{N_1^{(k)}}$, $\forall i$

STEP 5 If the error indicator (8) is such that $E_i^{(k)} > \tau$

then a refinement is applied around the point $\boldsymbol{x}_i^{(k)}$ to create

the sets $X^1_{N_1^{(k+1)}}$, $X^1_{N_2^{(k+1)}}$, $Z^1_{N_1^{(k+1)}}$ and $Z^1_{N_2^{(k+1)}}$

else set $k^* = k + 1$ and stop

STEP 6 Return the refined sets $X^1_{N_2^{(k^*)}}$ and $Z^1_{N_2^{(k^*)}}$

introduced. Although the associated collocation matrix has the same structure as in (11) and the blocks $(\hat{\Phi}_{\mathcal{L}_{II}})_{ij}$ and $(\hat{\Phi}_{BI})_{ij}$ are as in (12), the two remaining blocks $(\hat{\Phi}_{\mathcal{L}_{IB}})_{ij}$ and $(\hat{\Phi}_{BB})_{ij}$ are expressed in the following form

$$
\begin{aligned}
(\hat{\Phi}_{\mathcal{L}_{IB}})_{ij} &= \mathcal{L}\phi_\varepsilon(||\boldsymbol{x}_i^{(k)} - \boldsymbol{z}_j^{(k)}||_2), \qquad \boldsymbol{x}_i^{(k)} \in X^2_{N_I^{(k)}},\ \boldsymbol{z}_j^{(k)} \in Z^{2,e}_{N_B^{(k)}},\\
(\hat{\Phi}_{BB})_{ij} &= \phi_\varepsilon(||\boldsymbol{x}_i^{(k)} - \boldsymbol{z}_j^{(k)}||_2), \qquad \boldsymbol{x}_i^{(k)} \in X^2_{N_B^{(k)}},\ \boldsymbol{z}_j^{(k)} \in Z^{2,e}_{N_B^{(k)}}.
\end{aligned}
$$

As a result, the RBF approximate solutions $\hat{u}$ and $\hat{u}^e$ are obtained by using the same collocation points, while the centers turn out to be different. In fact, while the interior points in $Z^2_{N_I^{(k)}}$ and $X^2_{N_I^{(k)}}$ coincide for both systems, the boundary points in $Z^2_{N_B^{(k)}}$ (first system) and $Z^{2,e}_{N_B^{(k)}}$ (second system) are arranged on and outside the domain boundary, respectively. It is, however, important to observe that the number of boundary centers considered to find $\hat{u}$ is the same as external boundary ones used to compute the RBF solution $\hat{u}^e$.

After defining a set $Y^{(k)} = \{\boldsymbol{y}_1^{(k)}, \ldots, \boldsymbol{y}_{N^{(k)}}^{(k)}\}$ of *test* or *check points*, we validate the obtained results by means of the following error indicator

$$
I_i^{(k)} = |\hat{u}(\boldsymbol{y}_i^{(k)}) - \hat{u}^e(\boldsymbol{y}_i^{(k)})|, \qquad \boldsymbol{y}_i^{(k)} \in Y^{(k)}. \tag{13}
$$

Note that here the choice of check points is arbitrary. So, in order to validate the results, we might take scattered, quasi-random or other distributions of points. For this reason, our adaptive refinement is not mesh-based, but meshfree, since we have no assumption on the point refinement and no problem on the possible "distortion" of the original gridded structure of collocation points.

Now, fixed two tolerances (or thresholds) τ_{low} and τ_{upp}, such that $0 < \tau_{low} < \tau_{upp}$, for each iteration $k = 1, 2, \ldots$, if the indicator value $I_i^{(k)}$ in (13) is larger than τ_{upp}, we add the point $\boldsymbol{y}_i^{(k)}$ among the collocation points (and centers as well). Instead, if $I_i^{(k)}$ is smaller than τ_{low}, the test point is removed along with its nearest point. We can thus define the sets

$$
S_{T_{upp}^{(k)}} = \{\boldsymbol{y}_i^{(k)} \in Y^{(k)} \,:\, I_i^{(k)} > \tau_{upp},\, i = 1, \ldots, T_{upp}^{(k)}\}
$$

and

$$S_{T_{low}^{(k)}} = \{\bar{\boldsymbol{x}}_i^{(k)} \in X^2_{N^{(k)}} \,:\, I_i^{(k)} < \tau_{low},\, i = 1, \ldots, T_{low}^{(k)}\},$$

where $\bar{\boldsymbol{x}}_i^{(k)}$ is the point closest to $\boldsymbol{y}_i^{(k)}$, while $T_{upp}^{(k)}$ and $T_{low}^{(k)}$ denote the number of test points for which the indicator (13) is upper or lower than τ_{upp} and τ_{low}, respectively. Iteratively, for $k = 2, 3, \ldots$, we can therefore obtain a new set of discretization points

$$X^2_{N^{(k+1)}} = X^2_{N_I^{(k+1)}} \cup X^2_{N_B^{(k+1)}}, \quad \text{where} \quad X^2_{N_I^{(k+1)}} = (X^2_{N_I^{(k)}} \cup S_{T_{upp}^{(k)}}) \backslash S_{T_{low}^{(k)}},$$

and, accordingly, update the corresponding set $Z^2_{N^{(k+1)}}$ of centers defined similarly. The process stops when the set $S_{T_{low}^{(k)}}$ is empty. The iterative procedure concludes once the refinement process is completed, returning the final sets $X^2_{N^{(k^*)}}$ and $Z^2_{N^{(k^*)}}$ associated with the collocation solution $\hat{u}^e$, where k^* denotes the last iteration of the second phase. A pseudo-code of this second stage is sketched in Procedure 2. Therefore, the algorithm allows us to refine the set of collocation points when the error indicator (13) does not give us precise enough results, or coarsen the set of collocation points if the level of accuracy achieved is over the desired one. This process thus results in an addition or removal of points, thus making adaptive even this stage of the algorithm.

Procedure 2: Refinement technique based on the MARS scheme

STEP 1 Take the sets $X^1_{N_2^{(k^*)}}$ and $Z^1_{N_2^{(k^*)}}$ of collocation points and centers

from Procedure 1, assuming $X^2_{N^{(1)}} = X^1_{N_2^{(k^*)}}$ and $Z^2_{N^{(1)}} = Z^1_{N_2^{(k^*)}}$

STEP 2 Fix two tolerances τ_{low} and τ_{upp}, such that $0 < \tau_{low} < \tau_{upp}$

STEP 3 For $k = 1, 2, \ldots$ compute the k-th approximate solutions $\hat{u}$ and $\hat{u}^e$ via (3) (or (6))

constructed on the sets $X^2_{N^{(k)}}$ and $X^2_{N^{(k)}} \cup X^{2,e}_{N^{(k)}}$

STEP 4 Define a set $Y^{(k)}$ of test points

STEP 5 Evaluate the error at the test point $\boldsymbol{y}_i^{(k)} \in Y^{(k)}$ via indicator (13), $\forall i$

STEP 6 Construct the refined set

$$X^2_{N^{(k+1)}} = X^2_{N_I^{(k+1)}} \cup X^2_{N_B^{(k+1)}}, \quad \text{with} \quad X^2_{N_I^{(k+1)}} = (X^2_{N_I^{(k)}} \cup S_{T_{upp}^{(k)}}) \backslash S_{T_{low}^{(k)}}$$

where

$$S_{T_{upp}^{(k)}} = \{\boldsymbol{y}_i^{(k)} \in Y^{(k)} \,:\, I_i^{(k)} > \tau_{upp},\, i = 1, \ldots, T_{upp}^{(k)}\}$$

$$S_{T_{low}^{(k)}} = \{\bar{\boldsymbol{x}}_i^{(k)} \in X^2_{N^{(k)}} \,:\, I_i^{(k)} < \tau_{low},\, i = 1, \ldots, T_{low}^{(k)}\}$$

So if the error indicator

`i)` $I_i^{(k)} > \tau_{upp}$, add the test point $\boldsymbol{y}_i^{(k)}$ among the collocation points

`ii)` $I_i^{(k)} < \tau_{low}$, remove the collocation point $\bar{\boldsymbol{x}}_i^{(k)}$ nearest to $\boldsymbol{y}_i^{(k)}$

from the collocation points

Then the set $Z^2_{N^{(k+1)}}$ is updated

STEP 7 Stop when the set $S_{T_{low}^{(k)}}$ is empty

STEP 8 Return the final sets $X^2_{N^{(k^*)}}$ and $Z^2_{N^{(k^*)}}$ associated with $\hat{u}^e$

3.3. Complexity of the computational procedures

The first phase of our refinement technique is based on the AS scheme, in which we compare two approximate RBF solutions computed on coarser and finer sets of points via the error indicator (8). Nevertheless, this evaluation requires to solve two linear systems that involve the collocation matrices in (4) (or (7)). These numerical computations have a cost of $O(N^3)$ complexity. Obviously, this process is initially applied to the sets $X^1_{N_1^{(1)}}$, $X^1_{N_2^{(1)}}$, $Z^1_{N_1^{(1)}}$ and $Z^1_{N_2^{(1)}}$, but it has then to be iterated on the refined sets $X^1_{N_1^{(k)}}$, $X^1_{N_2^{(k)}}$, $Z^1_{N_1^{(k)}}$ and $Z^1_{N_2^{(k)}}$, for $k = 2, 3, \ldots$, till the stop criterion is satisfied.

In the second phase of the algorithm we apply the refinement procedure based on the MARS technique. Here, this computational approach is generally iterated a few times till the stop criteria are fulfilled. So we update step-by-step the sets $X^2_{N^{(k)}}$ and $Z^2_{N^{(k)}}$, for $k = 1, 2, \ldots$. It is, however, evident that the error indicator (13) needs to solve at each iteration two collocation problems, which are characterized by computation of the approximate solutions $\hat{u}$ and $\hat{u}^e$. At each iteration this requires to solve two collocation system of the form (4) (or (7)), whose order of computational cost is $O(M^3)$ and $O(M_e^3)$, respectively. Notice that here, M denotes the number of interior and boundary discretization points, while M_e identifies the same number that also includes external boundary points that are taken outside the domain Ω.

After determining the final collocation points, the adaptive refinement algorithm stops and the resulting approximate solution of the elliptic PDE problem can be computed on a set of evaluation points. This is done with a matrix-vector multiplication that returns a vector whose size is given by the final number of centers.

4. Numerical results and discussion

In this section we show some numerical results on the performance of the adaptive refinement algorithm described in Section 3. All the codes are implemented in MATLAB environment, while the experiments are carried out on a laptop with an Intel(R) Core(TM) i7-4500U CPU 1.80 GHz processor and 4GB RAM.

In the following we report the results obtained by the numerical solution of some benchmark elliptic Poisson-type problems with Dirichlet BCs of the form (1)–(2), with $\mathcal{L} = -\Delta$. In particular, in order to test more thoroughly our new adaptive scheme, we apply it to both nonsymmetric and symmetric RBF collocation methods discussed in Section 2. Acting in this way, we also have the chance to better analyze how the algorithm works in the different situations by changing the PDE problem. Moreover, in our test we focus on two RBFs of different smoothness such as M6 and M4 (see Table 1). The shape parameter ε is generally taken fixed, but in this work we also study the behavior of the numerical scheme when ε varies. From the numerical viewpoint it is indeed relevant to analyze what is the effect on the algorithm performance due to a change of the parameter ε. In fact, even if in this paper we are mainly interested in seeing how the new adaptive scheme works – and so not getting the best accuracy – from literature we know that the selection of the RBF shape parameter is a remarkable issue, since such a choice might even significantly influence the accuracy of the computational technique (see e.g. [10, 11]). As regards, then, the selection of the check points in Procedure 2, we use the sequence of Halton points [10]. It is however obvious that the choice of these validation points is arbitrary and so – as already remarked – other possible point distributions can be considered.

In the various tests we analyze the performance of our adaptive algorithm by considering four test problems of the form (1)–(2), defined both on the unit square domain $\Omega = [0, 1]^2$ on an irregular domain $\Omega \subset [0, 1]^2$. The exact solutions of such Poisson problems are given by

$$
\begin{aligned}
u_1(x_1, x_2) &= \sinh(0.3(4x_1 - 4)\sin(8x_2 - 4)\exp(-(4x_1 - 2.1)^4)), \\
u_2(x_1, x_2) &= \frac{1}{25(4x_1 - 2)^2 + 25(4x_2 - 2)^2 + 1}, \\
u_3(x_1, x_2) &= \tanh(15(x_2 - (0.4 + 0.2x_1))), \\
u_4(x_1, x_2) &= \frac{x_1^3 + x_2^3}{2} + \exp(-400(x_1 - 0.5)^2 - 400(x_2 - 0.5)^2).
\end{aligned}
$$

In Figure 2 we show a graphical representation of such analytic solutions defined on $\Omega = [0,1]^2$. Such problems are also studied in recent works (see e.g. [16, 20, 24]). They are good and diversified examples for testing new adaptive refinement algorithms.

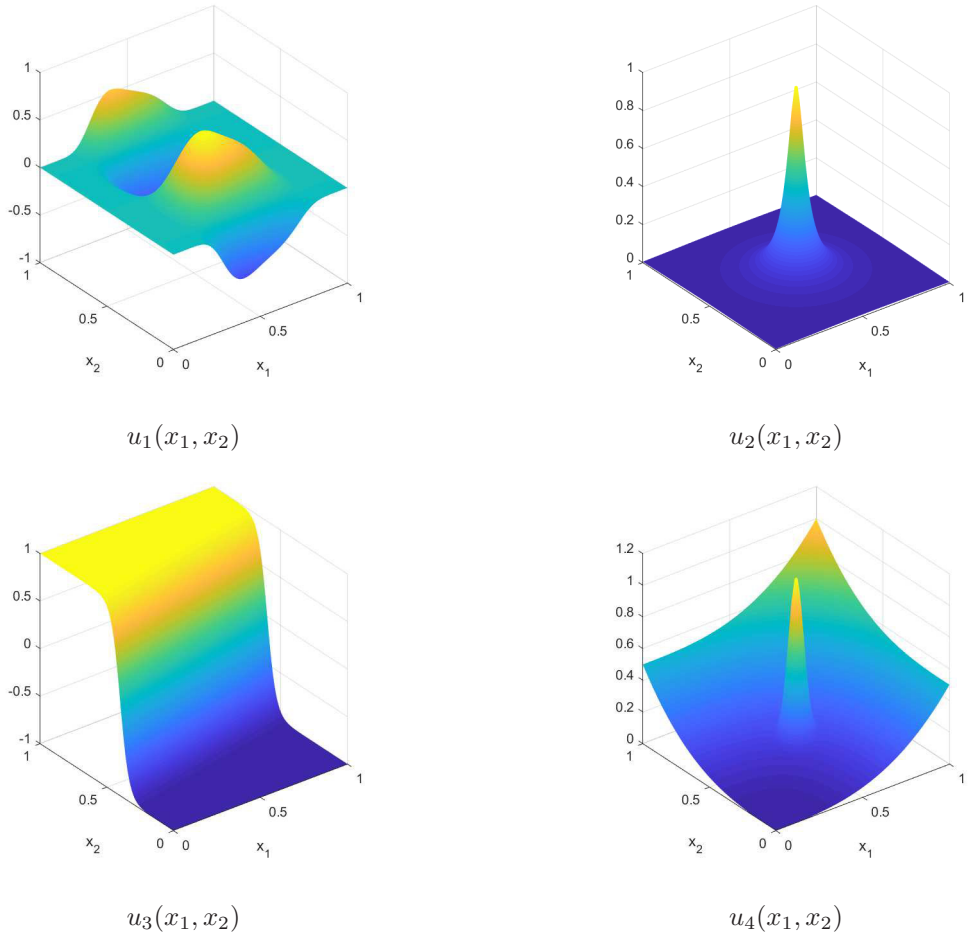

Figure 2: Exact solutions of PDE problems.

As a measure of the accuracy of the numerical results, we compute the Root Mean Square Error (RMSE) given by

$$\text{RMSE} = \sqrt{\frac{1}{N_{eval}} \sum_{i=1}^{N_{eval}} |u(\boldsymbol{\xi}_i) - \hat{u}(\boldsymbol{\xi}_i)|^2} = \frac{1}{\sqrt{N_{eval}}} ||u - \hat{u}||_2. \tag{14}$$

Here in (14) the evaluation error is carried out on a grid of $N_{eval} = 40 \times 40$ evaluation points, which are defined by $\boldsymbol{\xi}_i$, $i = 1, \ldots, N_{eval}$. Additionally, since we take an interest in analyzing the stability of RBF collocation methods, we report the Condition Number (CN) of the collocation matrix in (4) (or (7)) by making use of the MATLAB command `cond`.

Therefore, in order to numerically analyze the performance of our iterative algorithm on the unit square domain $\Omega = [0,1]^2$, we start the adaptive process by taking two sets of grid collocation points, which consist of $N_1^{(1)} = 529$ and $N_2^{(1)} = 1089$ interior and boundary points. In Table 2 we show a summary of results that we obtain by applying the nonsymmetric method and the symmetric one via M6 with $\varepsilon = 4$,

also providing the final number N_{fin} of discretization points used to get the final result. In particular, we note that the value of τ regarding the refinement phase based on the AS scheme is chosen on the basis of the considered test problem, whereas the lower and upper tolerances related to the MARS scheme are given by $(\tau_{low}, \tau_{upp}) = (10^{-8}, 10^{-4})$. Furthermore, Figures 3–4 show graphical representations of the final discretization points obtained for both Kansa's and Hermite-based approaches.

		Nonsymmetric			Symmetric		
Problem	τ	N_{fin}	RMSE	CN	N_{fin}	RMSE	CN
u_1	$1 \cdot 10^{-4}$	1139	2.53E−5	9.61E+12	1043	9.95E−5	2.79E+13
u_2	$2 \cdot 10^{-2}$	1513	1.80E−4	1.27E+13	1443	1.53E−4	6.13E+13
u_3	$5 \cdot 10^{-4}$	913	1.39E−4	8.33E+12	789	5.56E−4	2.34E+13
u_4	$5 \cdot 10^{-4}$	861	3.75E−4	7.47E+12	821	1.33E−3	3.45E+13

Table 2: Results obtained by applying the AS-MARS method via M6 with $\varepsilon = 4$ and $(\tau_{low}, \tau_{upp}) = (10^{-8}, 10^{-4})$. Tests have been carried out on the unit square domain.

From an analysis of these results, we observe as our algorithm works rather well for each of the problems studied, giving us back the expected level of accuracy. However, in general, from Table 2 it seems to be evident that Kansa's method provides slightly more precise results than Hermite approach. This fact is also proven by our further tests reported in Table 3, where we compare – for the sake of brevity only for the nonsymmetric method – the results obtained by varying the value of the shape parameter ε between 3 and 5 in the case of M6 and M4 basis functions. As regards the stability, we remark that the CN has a order of magnitude around 10^{+10}–10^{+13}. Although the RBF methods can suffer from severe ill-conditioning (in particular with very smooth kernels), the use of RBFs with limited smoothness along with the refinement strategies described in Section 3 allow us to keep under control the ill-conditioning avoiding the number of collocation points excessively grows. Then, from Figures 3–4 we can note as our adaptive scheme identifies clearly what are the areas that need to be refined. The main differences on the distribution of discretization points are essentially due to direct response of the numerical method with respect to the adaptive refinement technique. This is evident, for instance, if we compare Figures 3–4 on top-right, because in practice in Table 2 we do not observe significant changes in terms of both accuracy and stability. In addition, in order to conclude this study, in Figure 5 we report some graphs of the approximate RBF solution false colored by maximum absolute error.

In order to prove that our adaptive scheme is helpful, in Table 4 we show the results obtained in a specific case by applying the non-adaptive nonsymmetric (Kansa) and symmetric (Hermite) collocation schemes. In particular, here, for the sake of brevity we focus on the approximation of u_2 considering some sets of gridded points and using M6 with $\varepsilon = 4$. Comparing computational errors with those of Tables 2 and 3, on the one hand we can observe that a similar level of precision can be achieved only when we use more than 2000 collocation points. On the other hand, we note as with a similar number of points the accuracy in Table 4 is about one order of magnitude lower than the one obtained by our adaptive scheme (cf. Table 2).

Finally, we test our adaptive refinement algorithm considering the previous four Poisson-type problems on an irregular domain $\Omega \subset [0,1]^2$, which is bounded by the parametric curve [31]

$$\Gamma(\theta) = \frac{1}{9}\left(17 - 8\cos(3\theta)\right).$$

In these experiments we are also interested in showing that the combination between AS and MARS turns out to be advantageous in terms of accuracy. In particular, in Table 5 we compare the results obtained by applying the AS scheme (Procedure 1 only) and the AS-MARS (Procedure 1 + 2) via M6 with $\varepsilon = 4$. Lower and upper tolerances used in these tests are given by $(\tau_{low}, \tau_{upp}) = (10^{-8}, 10^{-5})$, while the initial numbers of gridded points are $N_1^{(1)} = 441$ and $N_2^{(1)} = 1089$. However, since these numbers refer to the points contained

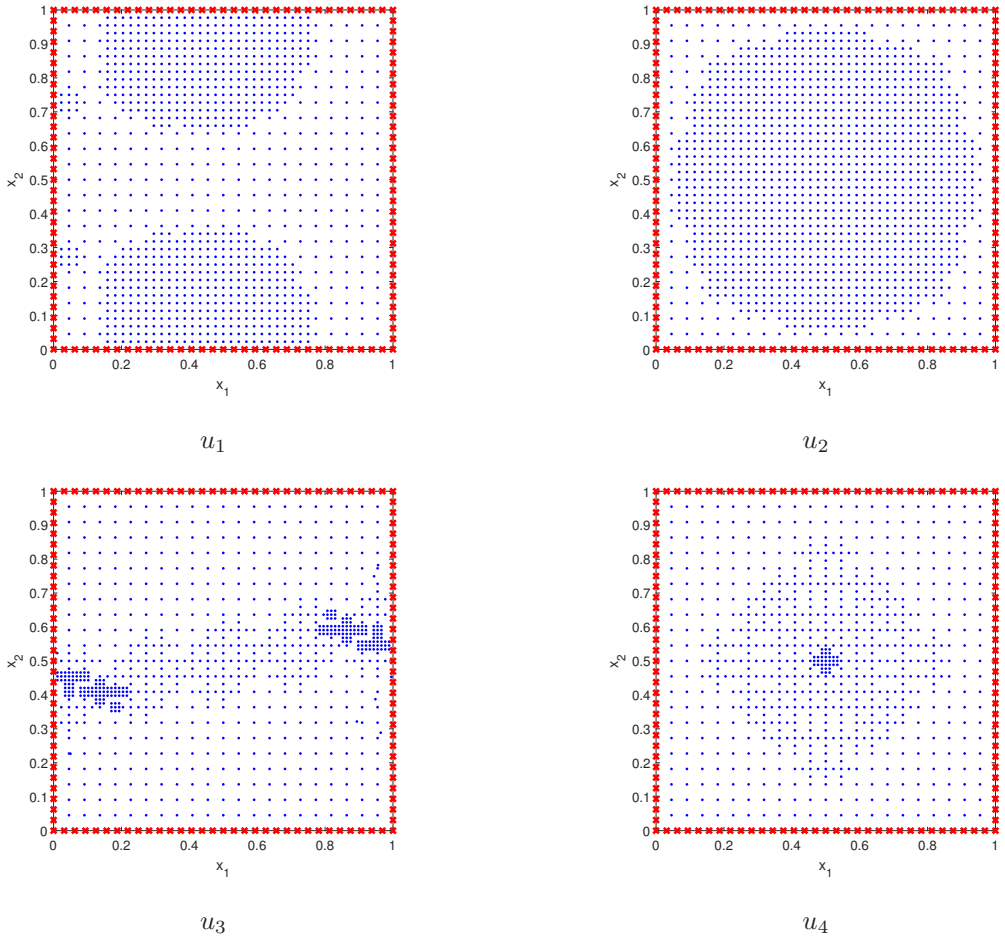

Figure 3: Final discretization points obtained by applying the AS-MARS scheme on the unit square domain. Tests have been carried out by using the nonsymmetric method via M6 with $\varepsilon = 4$.

in the unit square domain, the true initial numbers of points in the irregular shape domain are $N_1^{(1)} = 198$ and $N_2^{(1)} = 460$, with $N_{I_1}^{(1)} = 138$ and $N_{I_2}^{(1)} = 360$ gridded interior points, and $N_{B_1}^{(1)} = 60$ and $N_{B_2}^{(1)} = 100$ boundary points. All tests have been done by using Kansa's method. From Table 5 we can then remark as the AS-MARS method outperforms the AS scheme applied alone, enabling us to reduce the computational errors. This general benefit however results in a larger final number of collocation points and, obviously, slightly higher CNs and execution times (that are measured in seconds). The final discretization points obtained by applying the AS-MARS scheme are given in Figure 6.

5. Conclusions and future work

In this paper we presented a new adaptive refinement algorithm for solving elliptic Poisson-type PDE problems. This scheme is applied to Kansa's and Hermite-based methods. More precisely, the proposed algorithm is characterized by two stages. The first phase involves the AS scheme, where we compare two approximate RBF solutions that are computed on a coarser and a finer set of collocation points. The second phase is instead based on the MARS technique depending on an error indicator, which enables us an adaptive addition/removal of points on the basis of information extracted from error estimate.

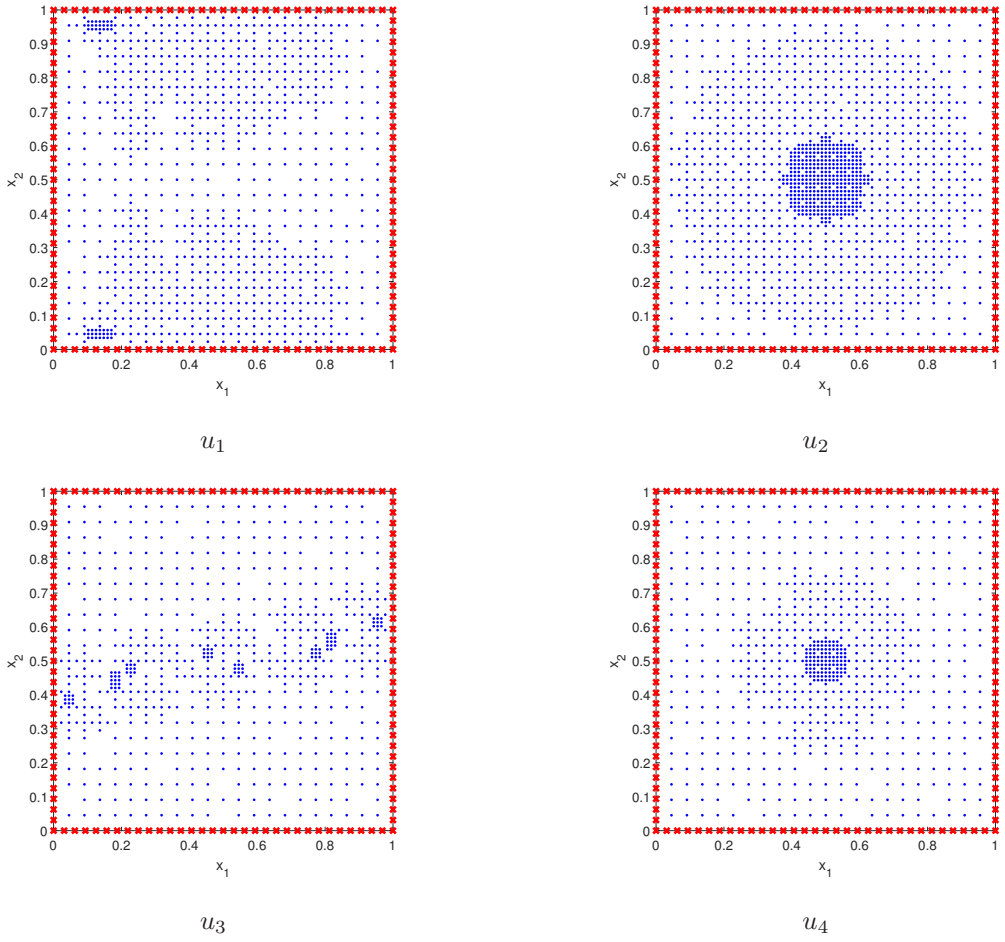

Figure 4: Final discretization points obtained by applying the AS-MARS scheme on the unit domain. Tests have been carried out by using the symmetric method via M6 with $\varepsilon = 4$.

As future work we propose to further improve our adaptive scheme to model other types of PDEs with any possible discontinuity or singularity. Additionally, since the method requires to solve two linear systems at each iteration to obtain the error indicators, its use turns out to be quite expensive in case of large scale problems. Further studies in this direction will therefore be necessary in future works.

Acknowledgments

The authors sincerely thank the two anonymous referees for their valuable comments and suggestions, which enabled to significantly improve the quality of this paper. They acknowledge support from the Department of Mathematics "Giuseppe Peano" of the University of Torino via Project 2019 "Mathematics for applications". Moreover, this work was partially supported by INdAM–GNCS Project 2019 "Kernel-based approximation, multiresolution and subdivision methods and related applications". This research has been accomplished within RITA (Research ITalian network on Approximation).

References

[1] M.D. Buhmann, Radial Basis Functions: Theory and Implementation, Cambridge Monogr. Appl. Comput. Math., vol. 12, Cambridge Univ. Press, Cambridge, 2003.

Problem	τ	ε	M6			M4		
			N_{fin}	RMSE	CN	N_{fin}	RMSE	CN
u_1	$1 \cdot 10^{-4}$	3	1075	4.08E−5	5.19E+13	1403	5.16E−5	1.03E+11
		4	1139	2.53E−5	9.61E+12	1415	5.18E−5	2.34E+10
		5	1159	2.61E−5	2.40E+12	1404	4.97E−5	1.05E+10
u_2	$2 \cdot 10^{-2}$	3	1512	1.79E−4	7.05E+13	1473	1.53E−4	1.34E+11
		4	1513	1.80E−4	1.27E+13	1473	1.53E−4	4.35E+10
		5	1512	1.79E−4	3.16E+12	1473	1.53E−4	1.77E+10
u_3	$5 \cdot 10^{-4}$	3	913	1.43E−4	4.71E+13	995	3.20E−4	7.96E+10
		4	913	1.39E−4	8.33E+12	1265	3.05E−4	3.40E+10
		5	913	1.34E−4	2.07E+12	1265	3.72E−4	1.37E+10
u_4	$5 \cdot 10^{-4}$	3	861	3.82E−4	4.01E+13	869	1.30E−3	7.52E+10
		4	861	3.75E−4	7.47E+12	895	1.28E−3	2.53E+10
		5	865	3.63E−4	1.95E+12	948	1.27E−3	1.07E+10

Table 3: Results obtained by applying the AS-MARS scheme to the nonsymmetric method and varying ε with $(\tau_{low}, \tau_{upp}) = (10^{-8}, 10^{-4})$. Tests have been carried out on the unit square domain.

N	RMSE [17]	RMSE [9]
1089	4.73e−3	4.70e−3
1444	1.21e−3	1.24e−3
1521	9.36e−4	9.12e−4
1600	6.95e−4	7.21e−4
2025	1.80e−4	1.78e−4

Table 4: Results obtained by applying the non-adaptive nonsymmetric [17] and symmetric [9] collocation methods for approximating u_2 on some sets of gridded points, and using M6 with $\varepsilon = 4$.

Problem	τ	AS method				AS-MARS method			
		N_{fin}	RMSE	CN	time	N_{fin}	RMSE	CN	time
u_1	$2 \cdot 10^{-4}$	246	4.44E−5	5.16E+14	1.0	347	2.06E−5	7.75E+14	1.3
u_2	$2 \cdot 10^{-2}$	473	4.64E−4	1.34E+15	1.7	650	4.16E−4	2.09E+15	4.7
u_3	$3 \cdot 10^{-4}$	629	7.47E−5	2.80E+15	2.4	838	6.12E−5	6.01E+15	8.3
u_4	$5 \cdot 10^{-4}$	582	4.55E−5	1.96E+15	1.0	610	4.36E−5	2.01E+15	2.4

Table 5: Comparison between results obtained by applying the AS scheme (Procedure 1 only) and the AS-MARS scheme (Procedure 1 + 2) by using M6 with $\varepsilon = 4$ and $(\tau_{low}, \tau_{upp}) = (10^{-8}, 10^{-5})$. Tests have been obtained by using the nonsymmetric method and on the irregular domain.

[2] R. Cavoretto, A. De Rossi, Adaptive meshless refinement schemes for RBF-PUM collocation, Appl. Math. Lett. 90 (2019) 131–138.

[3] R. Cavoretto, A. De Rossi, Error indicators and refinement strategies for solving Poisson problems through a RBF partition of unity collocation scheme, Appl. Math. Comput. 369 (2020), 124824.

[4] R. Cavoretto, A. De Rossi, An adaptive LOOCV-based refinement scheme for RBF collocation methods over irregular

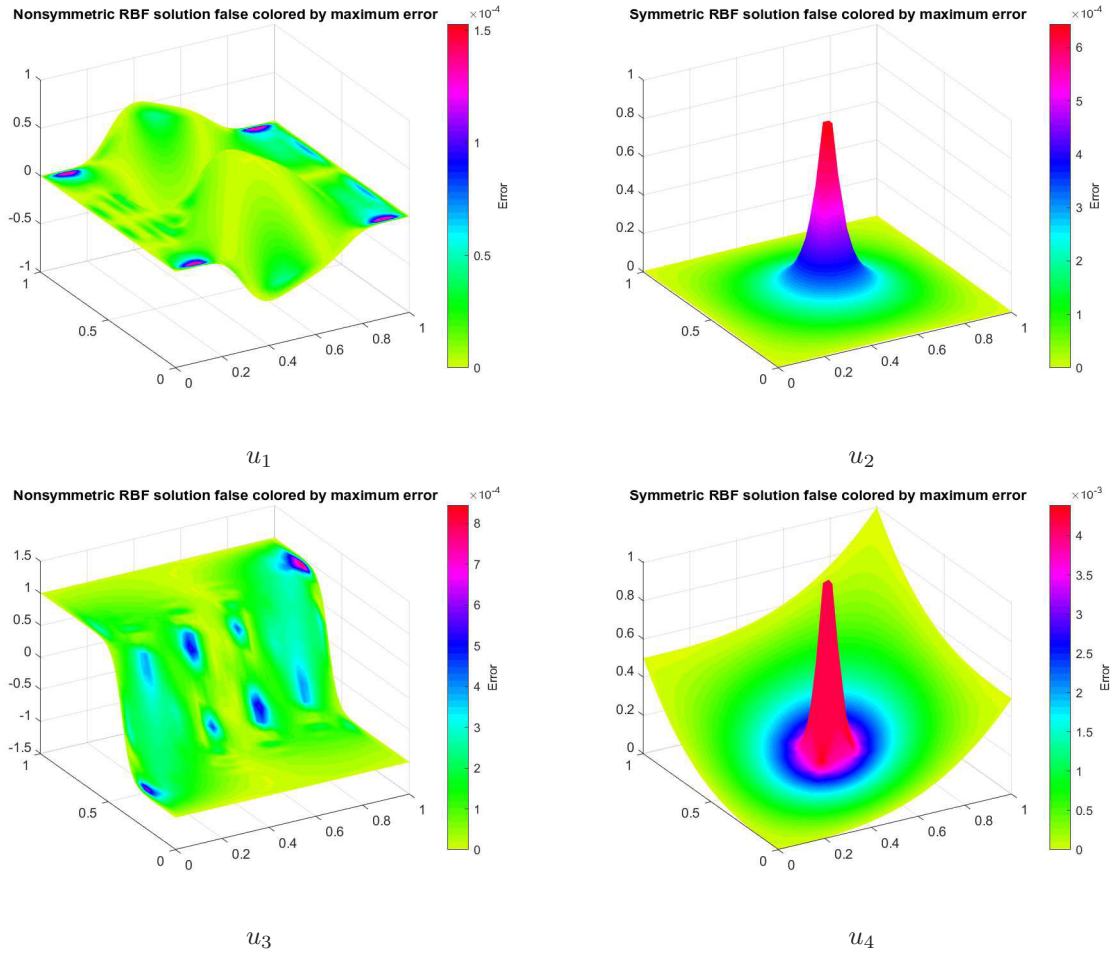

u_1 u_2

u_3 u_4

Figure 5: Examples of RBF solutions false colored by maximum error taken by Table 2.

domains, Appl. Math. Lett. 103 (2020), 106178.

[5] R. Cavoretto, A. De Rossi, A two-stage adaptive scheme based on RBF collocation for solving elliptic PDEs, Comput. Math. Appl. (2020), in press. https://doi.org/10.1016/j.camwa.2020.01.018

[6] W. Chen, Z.-J. Fu, C.S. Chen, Recent Advances on Radial Basis Function Collocation Methods, Springer Briefs in Applied Science and Technology, Springer, Heidelberg, 2014.

[7] O. Davydov, D.T. Oanh, Adaptive meshless centres and RBF stencils for Poisson equation, J. Comput. Phys. 230 (2011) 287–304.

[8] T.A. Driscoll, A.R.H. Heryudono, Adaptive residual subsampling methods for radial basis function interpolation and collocation problems, Comput. Math. Appl. 53 (2007) 927–939.

[9] G.E. Fasshauer, Solving partial differential equations by collocation with radial basis functions, in: Surface Fitting and Multiresolution Methods A. Le Méhauté, C. Rabut, L.L. Schumaker, eds., Vanderbilt Univ. Press, Nashville, TN, 1997, pp. 131–138.

[10] G.E. Fasshauer, Meshfree Approximation Methods with MATLAB, Interdisciplinary Mathematical Sciences, vol. 6, World Scientific Publishing Co., Singapore, 2007.

[11] G.E. Fasshauer, M.J. McCourt, Kernel-based Approximation Methods using MATLAB, Interdisciplinary Mathematical Sciences, Vol. 19, World Scientific Publishing Co., Singapore, 2015.

[12] A.I. Fedoseyev, M.J. Friedman, E.J. Kansa, Improved multiquadric method for elliptic partial differential equations via PDE collocation on the boundary, Comput. Math. Appl. 43 (2002) 439–455.

[13] B. Fornberg, N. Flyer, A Primer on Radial Basis Functions with Applications to the Geosciences, SIAM, Philadelphia, 2015.

[14] Y.C. Hon, R. Schaback, On unsymmetric collocation by radial basis functions, Appl. Math. Comput. 119 (2001) 177–186.

[15] M.A. Jankowska, A. Karageorghis, C.S. Chen, Improved Kansa RBF method for the solution of nonlinear boundary value

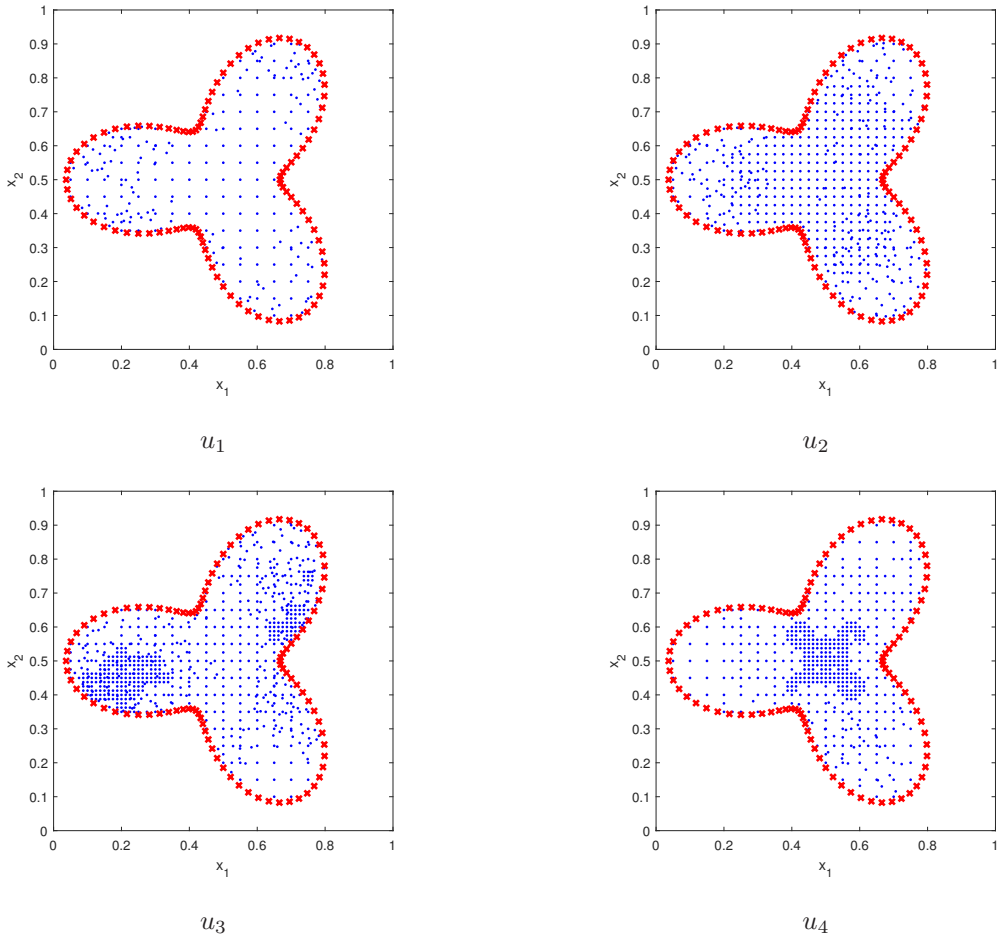

Figure 6: Final discretization points obtained by applying the AS-MARS scheme on the irregular domain. Tests have been carried out by using the nonsymmetric method via M6 with $\varepsilon = 4$.

problems, Eng. Anal. Bound. Elem. 87 (2018) 173–183.
[16] S. Kaennakham, N. Chuathong, An automatic node-adaptive scheme applied with a RBF-collocation meshless method, Appl. Math. Comput. 348 (2019) 102–125.
[17] E.J. Kansa, Multiquadrics–A scattered data approximation scheme with applications to computational fluid-dynamics–II solutions to parabolic, hyperbolic and elliptic partial differential equations, Comput. Math. Appl. 19 (1990) 147–161.
[18] G. Kosec, B. Šarler, H-adaptive local radial basis function collocation meshless method, CMC 26 (2011), 227–253.
[19] E. Larsson, B. Fornberg, A numerical study of some radial basis function based solution methods for elliptic PDEs, Comput. Math. Appl. 46 (2003) 891–902.
[20] E. Larsson, V. Shcherbakov, A. Heryudono, A least squares radial basis function partition of unity method for solving PDEs, SIAM J. Sci. Comput. 39 (2017) A2538–A2563.
[21] C.-F. Lee, L. Ling, R. Schaback, On convergent numerical algorithms for unsymmetric collocation, Adv. Comput. Math. 30 (2009) 339–354.
[22] M. Li, W. Chen, C.S. Chen, The localized RBFs collocation methods for solving high dimensional PDEs, Eng. Anal. Bound. Elem. 37 (2013) 1300–1304.
[23] H. Li, S.S. Mulay, Meshless Methods and Their Numerical Properties, 1st Edition, CRC Press, Boca Raton, FL, 2013.
[24] N.A. Libre, A. Emdadi, E.J. Kansa, M. Shekarchi, M. Rahimian, A fast adaptive wavelet scheme in RBF collocation for nearly singular potential PDEs, CMES Comput. Model. Eng. Sci. 38 (2008) 263–284.
[25] L. Ling, An adaptive-hybrid meshfree approximation method, Internat. J. Numer. Methods Engrg. 89 (2012) 637–657.
[26] L. Ling, R. Opfer, R. Schaback, Results on meshless collocation techniques, Eng. Anal. Bound. Elem. 30 (2006) 247–253.
[27] D.T. Oanh, O. Davydov, H.X. Phu, Adaptive RBF-FD method for elliptic problems with point singularities in 2D, Appl. Math. Comput. 313 (2017) 474–497.

[28] R. Schaback, Convergence of unsymmetric kernel-based meshless collocation methods, SIAM J. Numer. Anal. 45 (2007) 333–351.
[29] S.A. Sarra, Adaptive radial basis function methods for time dependent partial differential equations, Appl. Numer. Math. 54 (2005) 79–94.
[30] S.A. Sarra, E.J. Kansa, Multiquadric Radial Basis Function Approximation Methods for the Numerical Solution of Partial Differential Equations, Advances in Computational Mechanics, vol. 2, Tech Science Press, Encino, CA, 2009.
[31] S. Wei, W. Chen, Y. Zhang, H. Wei, R.M. Garrard, A local radial basis function collocation method to solve the variable-order time fractional diffusion equation in a two-dimensional irregular domain, Numer. Methods Partial Differential Eq. 34 (2018) 1209–1223.
[32] H. Wendland, Scattered Data Approximation, Cambridge Monogr. Appl. Comput. Math., vol. 17, Cambridge Univ. Press, Cambridge, 2005.
[33] T.-T. Wong, W.-S Luk, P.-A. Heng, Sampling with Hammersley and Halton points, J. Graphics Tools 2 (1997) 9–24.